

DISCOVERY OF A NEW SOFT GAMMA REPEATER, SGR 1627–41

PETER M. WOODS,¹ CHRYSSA KOUVELIOTOU,^{2,3} JAN VAN PARADIJS,^{1,4} KEVIN HURLEY,⁵ R. MARC KIPPEN,^{3,6}
MARK H. FINGER,^{2,3} MICHAEL S. BRIGGS,^{1,3} STEFAN DIETERS,^{1,3} AND GERALD J. FISHMAN³

Received 1999 March 17; accepted 1999 May 7; published 1999 May 28

ABSTRACT

We report the discovery of a new soft gamma repeater (SGR), SGR 1627–41, and present BATSE observations of the burst emission and *BeppoSAX* Narrow-Field Instrument observations of the probable persistent X-ray counterpart to this SGR. All but one burst spectrum are well fit by an optically thin thermal bremsstrahlung model with kT values between 25 and 35 keV. The spectrum of the X-ray counterpart, SAX J1635.8–4736, is similar to that of other persistent SGR X-ray counterparts. We find weak evidence for a periodic signal at 6.41 s in the light curve for this source. Like other SGRs, this source appears to be associated with a young supernova remnant, G337.0–0.1. Based upon the peak luminosities of bursts observed from this SGR, we find a lower limit on the dipole magnetic field of the neutron star of $B_{\text{dipole}} \geq 5 \times 10^{14}$ G.

Subject headings: stars: individual (SAX J1635.8–4736, SGR 1627–41) — stars: neutron — X-rays: bursts

1. INTRODUCTION

Soft gamma repeaters (SGRs) are a rare type of stellar object characterized by their transient emission of bursts of hard X-rays and soft γ -rays. Bursts have been detected from three such sources from 1979 (Mazets et al. 1981) until early 1998; two are in the Galactic plane (SGR 1806–20 and SGR 1900+14), and one is in the Large Magellanic Cloud (SGR 0526–66). One of the first SGR bursts detected, the famous 1979 March 5 burst from SGR 0526–66 (Mazets et al. 1979), provided a wealth of information about these sources (Thompson & Duncan 1995). This flare started with a short initial spike followed by a 3 minute train of coherent 8 s pulsations. A precise location of this burst was consistent with a young ($\sim 10^4$ yr) supernova remnant (SNR), N49 (Cline et al. 1982). The train of pulsations and the positional coincidence with the SNR indicated that the burst source is a young, magnetized neutron star.

Pointed X-ray observations of SGR burst location regions have shown that each SGR has associated with it a persistent X-ray source (Murakami et al. 1994; Hurley et al. 1999c; Rothschild, Kulkarni, & Ligenfelter 1994) within or near a young SNR (Kulkarni & Frail 1993; Hurley et al. 1999a; Cline et al. 1982). Furthermore, the persistent sources associated with the two Galactic SGRs are X-ray pulsars (Kouveliotou et al. 1998a; Hurley et al. 1999c) that show secular spin down at a rate $\sim 10^{-10}$ s s⁻¹ (Kouveliotou et al. 1998a, 1999). As argued by Thompson & Duncan (1996) and Kouveliotou et al. (1998a), this spin down is likely caused by magnetic dipole radiation, which implies a neutron star dipole magnetic field of $\sim 10^{14}$ – 10^{15} G. These results have provided strong observational evidence in support of the idea that SGRs are strongly magnetized neutron stars or “magnetars” (Duncan & Thompson 1992).

The majority of SGR bursts have durations less than 200 ms and are well characterized by optically thin thermal brems-

strahlung (OTTB) spectra with temperatures $kT \sim 30$ – 40 keV (Kouveliotou 1995). With the exception of the much more luminous March 5 event and a similar bright flare detected recently from SGR 1900+14 (Hurley et al. 1999d), SGR bursts reach peak luminosities up to $\sim 10^{42}$ ergs s⁻¹, far exceeding the Eddington luminosity for a $1.4 M_{\odot}$ neutron star. A statistical study of bursts from SGR 1806–20 has shown that no correlation exists between the energy released in a burst and the time until the next burst (Laros et al. 1987). A differential energy distribution of events follows a Gutenberg-Richter power law (-1.6 exponent; Gutenberg & Richter 1956) with a maximum energy $E_{\text{max}} \approx 5 \times 10^{41}$ ergs (Cheng et al. 1995). Each of these statistical properties are consistent with characteristics of earthquakes, which suggests that the SGR bursts may be triggered by neutron star crustquakes (Thompson & Duncan 1995).

Here, we report the discovery of SGR 1627–41, the first new SGR to be detected since 1979. We provide information on general burst characteristics and the persistent X-ray emission and draw comparisons to other SGRs. Like the other SGRs, this SGR is associated with a persistent X-ray source and the young SNR G337.0–0.1.

2. BATSE OBSERVATIONS

During a period of intense burst activity from SGR 1900+14, the Burst and Transient Source Experiment (BATSE; Fishman et al. 1989) trigger criteria were optimized to detect SGR burst events. On 1998 June 15, three consecutive BATSE-triggered bursts that were short in duration and had soft spectra originated from a region of the sky that was inconsistent with the three known SGR locations. Two days later, BATSE detected another 17 events from the same region, confirming the existence of a new SGR, SGR 1627–41 (Kouveliotou et al. 1998b; source name based upon initial BATSE location). Over the course of the next 6 weeks, a total of 99 bursts from this source were detected with BATSE, 39 of which triggered the instrument.

The bursts from SGR 1627–41 last between 25 ms and 1.8 s, with most burst durations clustering near 100 ms. In Figure 1, we show some representative burst profiles. This small sample shows the diverse temporal variability observed in bursts from this source. The longest event (Fig. 1*d*) is similar to two bursts seen from SGR 1900+14 with respect to both spectrum and temporal structure. These bursts are much longer

¹ Department of Physics, University of Alabama in Huntsville, Huntsville, AL 35899; peter.woods@msfc.nasa.gov.

² Universities Space Research Association.

³ NASA/Marshall Space Flight Center, ES-84, Huntsville, AL 35812.

⁴ Astronomical Institute “Anton Pannekoek,” University of Amsterdam, 403 Kruislaan, 1098 SJ Amsterdam, Netherlands.

⁵ Space Sciences Laboratory, University of California, Berkeley, Berkeley, CA 94720-7450.

⁶ Center for Space Plasma, Aeronomic, and Astrophysics Research, University of Alabama in Huntsville, Huntsville, AL 35899.

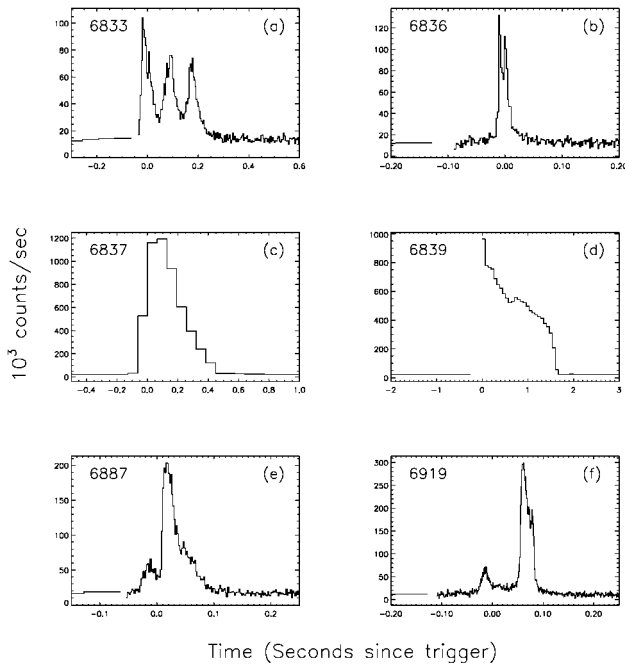


FIG. 1.—Sample of six bursts of SGR 1627–41 observed with the BATSE Large Area Detectors. The upper and lower panels are time-tagged event data (>25 keV) accumulated with (a) 4 ms, (b) 2 ms, (e) 2 ms, and (f) 1 ms time resolution. The middle panels are DISCRIMINATOR SCIENCE (DISCSC) data (>25 keV) accumulated with 64 ms time resolution. Trigger times for these six events are (a) 50,981.87322, (b) 50,982.03545, (c) 50,982.07120, (d) 50,982.16969, (e) 50,993.30911, and (f) 51,006.91017 in MJD (UT). BATSE trigger numbers are given in the upper left corner of each panel.

than typical SGR events and have very smooth temporal profiles with abrupt γ -ray emission start and end points.

Because of the rapid succession of bursts on June 17 and 18, only limited fine spectral data for a given trigger were read out from the spacecraft before the next trigger, making detailed spectral reconstruction impossible for most bursts. Of the 39 triggered bursts, fine spectral resolution data were available for only eight events, including two very bright bursts (Figs. 1c and 1d). We fit power-law, blackbody, and OTTB spectral models to those bursts and find that the OTTB model best represents the time-integrated burst spectra of the six dim events and one of the two bright bursts (Fig. 1d). The measured kT values of the six dim events range between 25 and 35 keV, having a weighted mean of 27 keV. The spectral form of these six events agrees well with previous modeling of burst spectra from the other three SGRs (see, e.g., Fenimore, Laros, & Ulmer 1994). The spectrum of the longer, bright burst (Fig. 1d) is consistent with the dimmer events, $kT = 27.0 \pm 0.4$ keV. Because of the excessive dead time of the BATSE detectors for the brightest burst (Fig. 1c), a detailed spectral deconvolution has not yet been performed. To first order, however, the time-integrated spectrum for this burst can be fit with a power-law model having a photon index $\alpha = -2.09 \pm 0.05$, which is much harder than any other emission detected from this SGR with BATSE.

In order to estimate the peak fluxes of a larger sample of bursts, we applied the OTTB model to bursts with coarse spectral resolution (four channels) and fair temporal resolution (64 ms). We assumed a fixed kT corresponding to the measured weighted mean value for the five dim events (27 keV) and allowed only the normalization (energy flux) to vary. One draw-

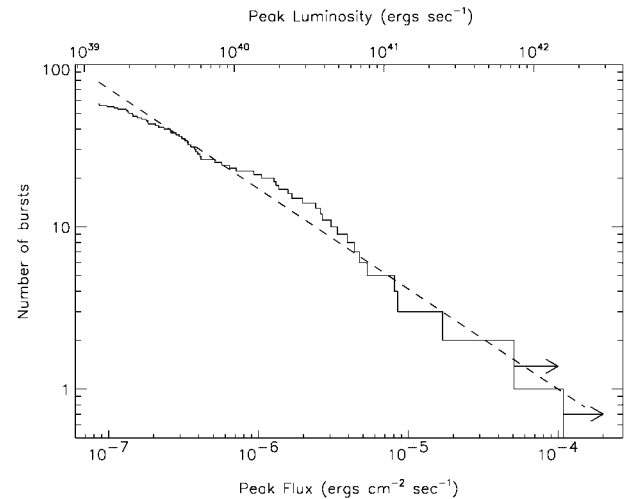


FIG. 2.—Cumulative peak flux (0.064 s) distribution for 57 events. The dashed line is a power-law fit to these data having an exponent equal to -0.62 . The bottom horizontal axis labels the peak flux, and the top horizontal axis gives the peak luminosity assuming isotropic emission and an 11 kpc distance to the source.

back to this method is that many bursts reach their peak flux for only a short time—less than 64 ms—so these peak flux measurements will underestimate the true peak flux for some events. Given the limited data availability, however, this timescale provided the largest sample of events. Figure 2 shows the cumulative peak flux distribution on the 64 ms timescale for 57 events. The observed peak fluxes range over 3 orders of magnitude between 9×10^{-8} and 1.1×10^{-4} ergs $\text{cm}^{-2} \text{s}^{-1}$. Dead-time effects for the two brightest events were excessive, so these peak flux measurements (1.1 and 0.51×10^{-4} ergs $\text{cm}^{-2} \text{s}^{-1}$) can be treated as lower limits. The dashed line represents a power-law fit to this distribution, which has an exponent $\gamma = -0.62 \pm 0.08$. No turnover is seen for this distribution out to 1.1×10^{-4} ergs $\text{cm}^{-2} \text{s}^{-1}$. We also constructed a cumulative burst fluence distribution for these events, which has a similar slope of $\gamma = -0.48 \pm 0.07$. The differential fluence (energy) distribution then has an exponent equal to -1.5 , which agrees well with the Gutenberg-Richter power-law index (-1.6). A number of factors may have artificially altered these two distributions. Dead-time problems for the brightest events would tend to bend each distribution down slightly at the larger peak flux/fluence values. Decreased trigger efficiency for the dim bursts will cause a turnover at the low end of each distribution. Assuming a fixed kT value may skew the distributions slightly. Also, nondetection of events due to Earth occultation of the source may alter the distribution for a small number of observed events. The above errors represent the 1σ statistical errors only and do not include uncertainties due to these systematic effects.

Using the BATSE triggers, the burst source was coarsely located (Kouveliotou et al. 1998b) at $\alpha = 16^{\text{h}}27^{\text{m}}$ and $\delta = -41^{\circ}$ (J2000) with an error circle of radius 2° . Detection of SGR events by both BATSE and the *Ulysses* spacecraft provided a narrow location annulus 1:7 wide (Hurley et al. 1998a). Using BATSE Earth occultation constraints, we limited the allowable range along the annulus to $1^{\circ}5$ (Woods et al. 1998; Fig. 3). A more detailed account of the localization of this SGR is reported in Hurley et al. (1999b) and Smith, Bradt, & Levine (1999). In view of the association of SGRs with young SNRs, we

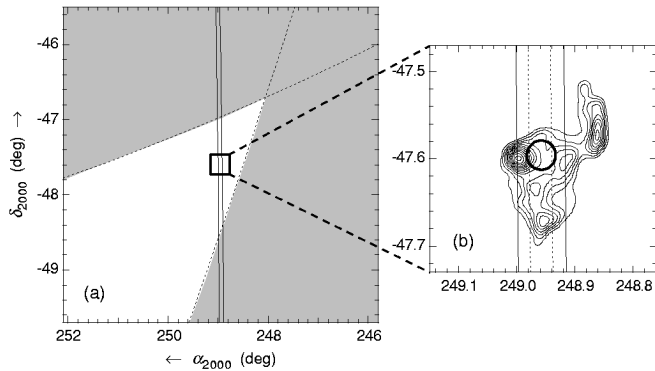


FIG. 3.—Localization of SGR 1627–41 and SAX J1635.8–4736. (a) Interplanetary Network (IPN) arc (solid lines) and Earth occultation constraints (shaded region). (b) Magnification of region near G337.0–0.1 (radio contours; Whiteoak & Green 1996). Solid straight lines represent BATSE-Ulysses IPN arc. Dotted lines are the Konus-Ulysses IPN arc (Hurley et al. 1998b). The circle represents error region for SAX J1635.8–4736.

searched the Whiteoak & Green (1996) catalog of SNRs near the refined error box. A single SNR, G337.0–0.1 (Sarma et al. 1997), was found (Woods et al. 1998) within the $1'.5 \times 1'.7$ error box. With hopes of detecting an X-ray counterpart for this SGR, a target-of-opportunity observation of this SNR was initiated using the *BeppoSAX* (Boella et al. 1997a) Narrow-Field Instruments.

3. *BeppoSAX* OBSERVATIONS

Two observations of SNR G337.0–0.1 were performed on 1998 August 7 and again on September 16. These observations revealed a previously undetected X-ray source (SAX J1635.8–4736) at $\alpha = 16^{\text{h}}35^{\text{m}}49^{\text{s}}.8$ and $\delta = -47^{\circ}35'44''$ (J2000) with an error circle of radius $1'$ (95% confidence; Fig. 3), consistent with the SNR location. A known source, 4U 1630–472, is also seen near the edge of the field of view for each observation. A light curve of the new source for each observation does not show any burst activity, which is consistent with BATSE observations for those time periods. Using the Low-Energy Concentrator Spectrometer (Parmar et al. 1997) and two Medium-Energy Concentrator Spectrometers (MECSs; Boella et al. 1997b), we fit the spectrum of SAX J1635.8–4736 from 0.1 to 10 keV. The spectrum is well represented by a power law with interstellar absorption. Under the assumption that the spectral form (i.e., the power-law index and hydrogen column density) remains constant between observations, we fit the observations simultaneously, allowing only the normalization to vary between the two. We get an acceptable fit with a reduced χ^2 value of 0.92 for 160 degrees of freedom and find a power-law (photon) index $\alpha = -2.5 \pm 0.2$ and a column density $N_{\text{H}} = (7.7 \pm 0.8) \times 10^{22} \text{ cm}^{-2}$. The unabsorbed flux (2–10 keV) declines between the observations (40.3 days) from $(6.7 \pm 0.3) \times 10^{-12}$ to $(5.2 \pm 0.4) \times 10^{-12} \text{ ergs cm}^{-2} \text{ s}^{-1}$. Assuming that this source is located within the SNR, the distance is 11 kpc (Sarma et al. 1997). The source luminosity is then 9.7×10^{34} and $7.6 \times 10^{34} \text{ ergs s}^{-1}$ for the two observations.

Using standard *BeppoSAX* analysis techniques, source counts were extracted from the combined MECS units for SAX J1635.8–4736 and binned at 0.5 s time resolution. We then performed a fast Fourier transform of the 1998 August light curve, searching frequencies from 0 to 1 Hz, and found that the largest value in the power density spectrum was at 0.156

Hz. Although not very significant by itself, the corresponding period falls within the tight range of observed periods (5–8 s) for the other SGRs. Using the barycenter-corrected time tags, we ran an epoch-fold search about the period corresponding to the highest power, which revealed a marginally significant peak (6×10^{-3} chance probability taking into account the number of trials; 1500 between 6.38 and 6.44 s) at 6.41318(3) s (JD = 2,451,032.5). The nearly sinusoidal pulse profile has an rms pulse fraction of $10.0\% \pm 2.6\%$. We performed the same analysis on the 1998 September observation, but did not find any significant peak in the power density spectrum near 0.156 Hz or anywhere else between 0 and 1 Hz. However, given the weak signal found in August and the fact that 45% fewer source counts were recorded in the MECS units during the September observation, we would not expect to find this pulsed signal.

4. DISCUSSION

We propose that SAX J1635.8–4736 is the X-ray counterpart to SGR 1627–41. There are a number of observations discussed here that support this claim. First, the position of SAX J1635.8–4736 is mutually consistent with the narrow error box for SGR 1627–41 (Hurley et al. 1999b; Smith et al. 1999) and the SNR G337.0–0.1. Second, its spectrum is very similar to those found for the other SGR X-ray counterparts (Hurley et al. 1999c). Also, this X-ray source is variable near a burst active period for SGR 1627–41, which has also been found for the X-ray counterpart of SGR 1900+14 (Hurley et al. 1999c; Murakami et al. 1999; Woods et al. 1999). Furthermore, the X-ray flux from the SNR would not be expected to vary; therefore, the variable X-ray source must be associated with something other than the SNR, i.e., the SGR. Finally, the marginal detection of pulsations at 6.4 s, if confirmed, would agree well with the known spin periods of the three other SGRs that fall within a tight range of 5–8 s (Kouveliotou et al. 1998a; Hurley et al. 1999c; Mazets et al. 1979).

For the distance of 11 kpc, G337.0–0.1 has a small diameter of $\sim 5 \text{ pc}$ (Sarma et al. 1997). There are only a few SNRs this small (see Case & Bhattacharya 1998), and a large fraction of them are very young (e.g., Tycho, Kepler, Cas A). This suggests that G337.0–0.1 is also very young. The association of SGR 1627–41 with G337.0–0.1 strengthens the connection between SGRs and young SNRs.

Given the distance to the SNR G337.0–0.1 and assuming isotropic emission, the burst peak luminosities ($>25 \text{ keV}$) vary from 10^{39} to $10^{42} \text{ ergs s}^{-1}$ (Fig. 2). Paczyński (1992) suggested that SGR 0526–66 may have a critical luminosity $\sim 2 \times 10^{42} \text{ ergs s}^{-1}$, based upon the tail of the March 5 event and the subsequent bursts detected over the following years. The much brighter initial spike ($\sim 5 \times 10^{44} \text{ ergs s}^{-1}$) of the March 5 event may possibly be interpreted as a bright magnetic flare from low optical depth (Paczyński 1992) or a relativistically expanding fireball from the stellar surface (Thompson & Duncan 1995) in the context of this argument. Paczyński calculated the relation between the dipole magnetic field (B_{dipole}) of a neutron star and the critical luminosity (L_{crit}) the magnetosphere will allow to escape in the limit in which $L_{\text{crit}} \gg L_{\text{Edd}}$ (L_{Edd} is the standard Eddington luminosity for a $1.4 M_{\odot}$ neutron star). This relation is given by

$$\frac{L_{\text{crit}}}{L_{\text{Edd}}} \approx 2 \left(\frac{B_{\text{dipole}}}{10^{12} \text{ G}} \right)^{4/3} \left(\frac{g}{2 \times 10^{14} \text{ cm s}^{-2}} \right)^{-1/3},$$

where g is the surface acceleration due to gravity. For SGR

0526–66, Paczyński found a dipole magnetic field of $\sim 6 \times 10^{14}$ G, which is consistent with independent estimates made by Duncan & Thompson (1992). The maximum observed peak luminosity from SGR 1806–20 is 1.8×10^{42} ergs s^{-1} (Fenimore et al. 1994). Again, this corresponds to a magnetic field of $\sim 6 \times 10^{14}$ G. This agrees well with the measurement of $B_{\text{dipole}} \approx 8 \times 10^{14}$ G reported by Kouveliotou et al. (1998a), which is based upon the spin-down of the pulsar associated with SGR 1806–20. For SGR 1627–41, we do not detect a turnover in the cumulative peak luminosity distribution, but we can place a lower limit on this value of 1.6×10^{42} ergs s^{-1} based upon the highest observed peak luminosity. Assuming that the radiation from these bursts originates near the stellar surface, the lower limit on the magnetic field of the presumed magnetar associated with SGR 1627–41 is $B_{\text{dipole}} \geq 5 \times 10^{14}$ G. This estimate may be confirmed with the definitive

measurement of a pulse period and its derivative for SGR 1627–41.

We are grateful to the referee of this manuscript, who provided constructive criticism and good suggestions. We thank other BATSE team members for useful discussions of dead-time effects of the instrument. This research has made use of SAXDAS linearized and cleaned event files produced at the *BeppoSAX* Science Data Center. We would also like to thank Lorella Angelini for her assistance with analyzing the *BeppoSAX* data. The Molonglo Observatory Synthesis Telescope is operated by the University of Sydney with support from the Australian Research Council and the Science Foundation for Physics within the University of Sydney. P. M. W. acknowledges support from NASA through grant NAG5-3674. J. v. P. acknowledges support from NASA through grants NAG5-3764, NAG5-7060, and NAG5-7808.

REFERENCES

- Boella, G., Butler, R. C., Perola, G. C., Piro, L., Scarsi, L., & Bleeker, J. A. M. 1997a, *A&AS*, 122, 299
 ———. 1997b, *A&AS*, 122, 327
 Case, G., & Bhattacharya, D. 1998, *ApJ*, 504, 761
 Cheng, B., Epstein, R. I., Guyer, R. A., & Young, C. 1995, *Nature*, 382, 518
 Cline, T. L., et al. 1982, *ApJ*, 255, L45
 Duncan, R., & Thompson, C. 1992, *ApJ*, 392, L9
 Fenimore, E. E., Laros, J. G., & Ulmer, A. 1994, *ApJ*, 432, 742
 Fishman, G. J., et al. 1989, *Compton Observatory Science Workshop*, ed. W. N. Johnson (NASA Conf. Publ.; Washington, DC: NASA), 2
 Gutenberg, B., & Richter, C. F. 1956, *Bull. Seism. Soc. Am.*, 46, 105
 Hurley, K., Kouveliotou, C., Kippen, M., & Woods, P. 1998a, *IAU Circ.* 6948
 Hurley, K., Kouveliotou, C., Woods, P., Cline, T., Butterworth, P., Mazets, E., Golenetskii, S., & Frederics, D. 1999a, *ApJ*, 510, L107
 Hurley, K., Kouveliotou, C., Woods, P., Mazets, E., Golenetskii, S., Cline, T., & van Paradijs, J. 1999b, *ApJ*, 519, L143
 Hurley, K., et al. 1998b, *IAU Circ.* 6966
 ———. 1999c, *ApJ*, 510, L111
 ———. 1999d, *Nature*, 397, 41
 Kouveliotou, C. 1995, *Ap&SS*, 231, 49
 Kouveliotou, C., et al. 1998a, *Nature*, 393, 235
 Kouveliotou, C., Kippen, M., Woods, P., Richardson, G., Connaughton, V., & McCollough, M. 1998b, *IAU Circ.* 6944
 Kouveliotou, C., et al. 1999, *ApJ*, 510, L115
 Kulkarni, S., & Frail, D. 1993, *Nature*, 365, 33
 Laros, J., et al. 1987, *ApJ*, 320, L111
 Mazets, E. P. 1979, *Nature*, 282, 587
 ———. 1981, *Ap&SS*, 80, 3
 Murakami, T., Kubo, S., Shibasaki, N., Takeshima, T., Yoshida, A., & Kawai, N. 1999, *ApJ*, 510, L119
 Murakami, T., Tanaka, Y., Kulkarni, S. R., Ogasaka, Y., Sonobe, T., Ogawara, Y., Aoki, T., & Yoshida, A. 1994, *Nature*, 368, 127
 Paczyński, B. 1992, *Acta Astron.*, 42, 145
 Parmar, A. N., et al. 1997, *A&AS*, 122, 309
 Rothschild, R., Kulkarni, S., & Lingenfelter, R. 1994, *Nature*, 368, 432
 Sarma, A., Goss, W., Green, A., & Frail, D. 1997, *ApJ*, 483, 335
 Smith, D., Bradt, H., & Levine, A. 1999, *ApJ*, 519, L147
 Thompson, C., & Duncan, R. 1995, *MNRAS*, 275, 255
 ———. 1996, *ApJ*, 473, 322
 Whiteoak, J., & Green, A. 1996, *A&AS*, 118, 329
 Woods, P., Kippen, M., van Paradijs, J., Kouveliotou, C., McCollough, M., & Hurley, K. 1998, *IAU Circ.* 6948
 Woods, P., Kouveliotou, C., van Paradijs, J., Finger, M., & Thompson, C. 1999, *ApJ*, 518, L103